

# Thermal Contrast Model for Optical Gas Imaging Performance Analysis

Robert Olbrycht

Lodz University of Technology, Institute of Electronics, Al. Politechniki 8, 93-590 Lodz, Poland

**Abstract:** The paper presents numerical modelling of thermal contrast in optical gas imaging (OGI) applications. The physical temperature of an imaged gas plume may be either higher or lower than the background, and this difference is a necessary condition for detection. Depending on the actual thermal contrast between the plume and the background, the measured temperature difference will vary. Ideally, this contrast should be as large as possible to ensure clear plume visualization. In practice, however, one must adapt to real world conditions and be able to predict the expected measured temperature difference and compare it with the camera's Noise Equivalent Temperature Difference (NETD) to estimate the signal to noise ratio. According to the results presented in this study, due to the combined effects of Planck's law, the camera's radiometric response, and gas absorption spectra, the measured thermal contrast strongly depends on the absolute physical temperatures of both the gas and the background—not only on the temperature difference between them.

**Keywords:** thermal imaging, optical gas imaging, camera, thermal contrast

## 1. Introduction

Optical gas imaging (OGI) is a technique established in industry and environment protection, used to detect gas leaks from process installations, tanks, dumps or several other types of sources. It is based on the ability of certain gases to absorb or emit infrared radiation, depending on their temperature, thus providing thermal contrast between the gas plume and the background area of the scene [1, 2]. The principle of optical gas imaging is presented in Fig. 1.

In the area of the scene, where a gas cloud is present, the camera Focal Plane Array (FPA) will receive radiation being the sum of the radiation emitted by the gas cloud ( $M_{gas}$ ) and the background radiation transmitted through the gas cloud ( $M_T$ ). In the area of the scene where no gas is present, the background radiation  $M_{bkg}$  will reach the FPA. Thus, to be able to detect the gas in ideal conditions, formula (1) needs to be fulfilled [2].

$$\left| T(M_{bkg}) - T(M_{gas} + M_T) \right| > NETD \quad (1)$$

where:  $NETD$  – noise equivalent temperature difference of the camera;  $M_{bkg}$  – background radiation intensity;  $M_T$  – radiation

intensity transmitted through the gas cloud;  $M_{gas}$  – radiation intensity emitted by the gas cloud;  $T(M_x)$  – temperature equivalent to the radiation intensity  $I_x$ , according to the camera calibration curve.

According to formula (1), a temperature difference between the background and the gas leak, as measured by the camera, exceeding the camera noise is needed to be able to spot the leak. The higher will be that difference, the easier will be to detect leaks. For clarity, further in the text, the thermal contrast term will be used to describe the difference between the background temperature and the gas plume temperature, as measured by the camera, whereas the term of temperature difference will be used to describe the difference between the physical background and gas temperature.

There is no universal rule that can provide the lowest temperature difference necessary to guarantee gas detection. It depends on many factors, such as camera sensitivity, gas type and concentration, temperature, leak size and finally the camera operator experience [3]. What is more, the temperature contrast measured by the camera is typically much lower than the temperature difference between the gas and the background. This is because gas absorption spectral bands are usually considerably narrower than typical thermographic cameras spectral sensitivity bands. This problem may be mitigated by the use of bandpass interference filters [2].

In this paper a thermal contrast model based on radiance calculations is proposed, in order to calculate the temperature difference between the gas plume and the background needed to detect leaks. In case of presented examples, a general purpose cooled thermographic camera operating in the MWIR band (3–5  $\mu\text{m}$ ) is used without any bandpass filters limiting its spectral sensitivity bandwidth.

### Autor korespondujący:

Robert Olbrycht, robert.olbrycht@p.lodz.pl

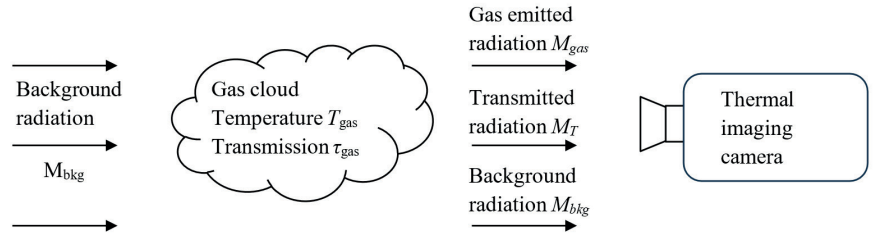
### Artykuł recenzowany

nadesłany 23.07.2025 r., przyjęty do druku 27.01.2026 r.



Zezwala się na korzystanie z artykułu na warunkach licencji Creative Commons Uznanie autorstwa 4.0 Int.

Fig. 1. Principle of optical gas imaging  
Rys. 1. Zasada optycznego obrazowania gazów



## 2. Thermal contrast model

### 2.1. Radiance calculation

The aim of the proposed model is to allow calculations of the expected thermal contrast between background and gas, as measured by the camera, based on their physical temperature difference. According to formula (1), the value of the calculated thermal contrast should exceed *NETD* to be able to detect a leak in perfect conditions. In practice, however, it is advised that this thermal contrast is a few times greater than *NETD* to increase the chances of gas plume detection. The proposed model assumes that radiation emitted by the gas  $M_{gas}(T_{gas})$  and the background radiation  $M_{bkg}(T_{bkg})$  are independently calculated based on the Planck's Law (2).

$$M(T, \lambda) = \frac{2hc^2}{\lambda^5 \left( e^{\frac{hc}{\lambda kT}} - 1 \right)} \quad (2)$$

where:  $M(T, \lambda)$  – spectral radiance of blackbody,  $W \cdot m^{-3}$ ;  $T$  – temperature of blackbody, K;  $\lambda$  – wavelength, m;  $h$  – Planck constant  $6.62607015 \cdot 10^{-34} J \cdot s$ ;  $k$  – Boltzmann constant  $1.380649 \cdot 10^{-23} J \cdot K^{-1}$ ;  $c$  – speed of light  $299\,792\,458 m \cdot s^{-1}$ .

Because the gas is imaged against the background (bkg), its in-band radiance  $M_{gb}$  reaching the camera FPA needs to be calculated using formula (4), where  $\tau_{gas}$  stands for infrared transmission factor of this gas, which is highly dependent on

the wavelength. The same goes for the camera detector absorption characteristics  $\alpha_{det}$  – its impact also needs to be taken into account. For the sake of clarity, the formula for background radiance is also provided in the form (3).

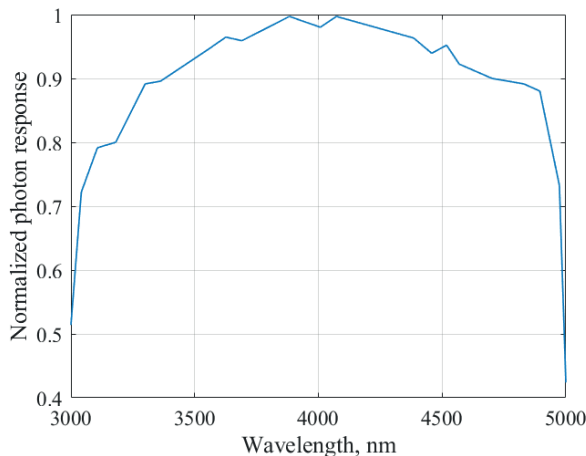
$$M_{bkg} = \int_{\lambda_{min}}^{\lambda_{max}} \alpha_{det} M(T) d\lambda \quad (3)$$

$$M_{gb} = \int_{\lambda_{min}}^{\lambda_{max}} (1 - \tau_{gas}) \alpha_{det} M_{gas} d\lambda + \int_{\lambda_{min}}^{\lambda_{max}} \alpha_{det} \tau_{gas} M_{bkg} d\lambda \quad (4)$$

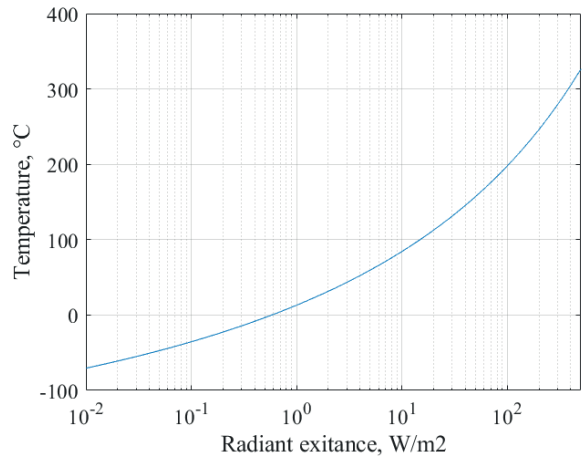
There is no need to include in the model the spectral transmission characteristics of the camera lens, but only in case it is approximately flat in the range covered by the detector spectral sensitivity. Camera calibration curve already takes into account the attenuation of the lens. Keeping the assumption of flat lens spectral transmission characteristics, one can assume that lowering its transmission will only increase the *NETD* of the camera. If the lens exhibits not flat spectral characteristics, it may impact the thermal contrast in the similar way as using an interference filter in the optical path [4]. This aspect, however, is beyond the scope of this paper, as it is focused on modelling the performance of a general purpose thermal imaging camera, not the one dedicated for optical gas imaging.

### 2.2. Radiometric response curve calculation

The next step requires calculation of the camera radiometric response curve  $T(M)$ , where the response to radiant exi-



a)



b)

Fig. 2. a) Normalized spectral photon response of a typical InSb detector [9], included in calculation of b) camera radiometric response curve scaled in temperature

Rys. 2. a) Znormalizowana widmowa odpowiedź typowego detektora fotonowego InSb [9], uwzględniona w obliczeniu b) charakterystyki radiometrycznej odpowiedzi kamery w skali temperatury

tance  $M$  is scaled in temperature  $T$  [5]. This is a simplification of the real case, where camera radiometric response curve is scaled in digital units – then it should be generally linear and an additional curve (non-linear calibration curve [6]) is used to recalculate these digital units to temperature. To calculate the camera radiometric response curve, one can use the formula (3), which includes the detector spectral sensitivity characteristics  $\alpha_{det}$  – for the purpose of this model, a typical InSb spectral response curve is taken, as shown in Fig. 2a [9]. Using the formula (3) for a set of desired temperature values results in the plot as shown in Fig. 2b.

### 2.3. Thermal contrast calculation

To calculate the thermal contrast, one needs to perform calculations for a set of chosen background temperature values and a set of chosen gas temperature values, using formulas given in subsection 2.1. When  $M_{bkg}$  and  $M_{gb}$  is found for a certain background temperature  $T_{bkg}$ , one needs to subtract this temperature from temperature  $T_{gb}$  obtained with camera radiometric response curve:  $T_{gb}(M_{gb})$ .

## 3. Model calculation results

The approach given in the previous section is used to calculate the thermal contrast, as seen by a thermographic camera, for different gas and background temperature values. For the purpose of calculations, a cooled FPA thermal camera operating in the 3–5  $\mu\text{m}$  (MWIR) infrared range, without bandpass filter, is taken. Two different gases are taken into consideration: carbon dioxide ( $\text{CO}_2$ ) and methane ( $\text{CH}_4$ ). Their infrared transmission spectra, presented in Fig. 3, were calculated based on the HITRAN (high-resolution transmission molecular absorption) model [10], assuming 100 % gas concentrations and a 1 cm optical path length.

A series of camera thermal contrast curves was calculated, for different background and gas temperature combinations, for carbon dioxide and methane. The results are shown in Fig. 4. Whereas in all cases a 100 % gas concentration and a 1 cm optical path length in the gas were assumed, other conditions could be introduced in the simulations based on the Beer-Lambert law, as discussed in [1, 7].

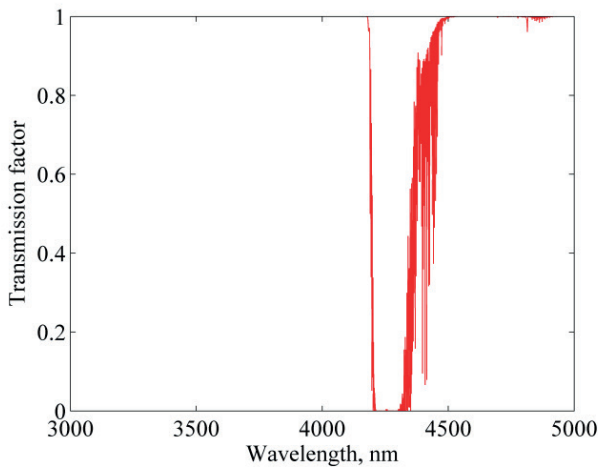
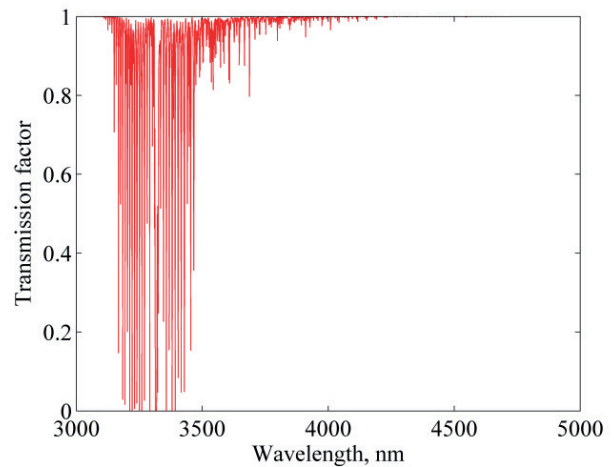
a)  $\text{CO}_2$ b)  $\text{CH}_4$ 

Fig. 3. Spectral transmission plots for a)  $\text{CO}_2$ , b)  $\text{CH}_4$  assuming 100 % gas concentration and a 1 cm path length, generated with HITRAN model  
Rys. 3. Wykresy transmisji widmowej dla a)  $\text{CO}_2$ , b)  $\text{CH}_4$ , przy założeniu 100 % stężenia gazu i długości ścieżki 1 cm, wygenerowane z modelu HITRAN

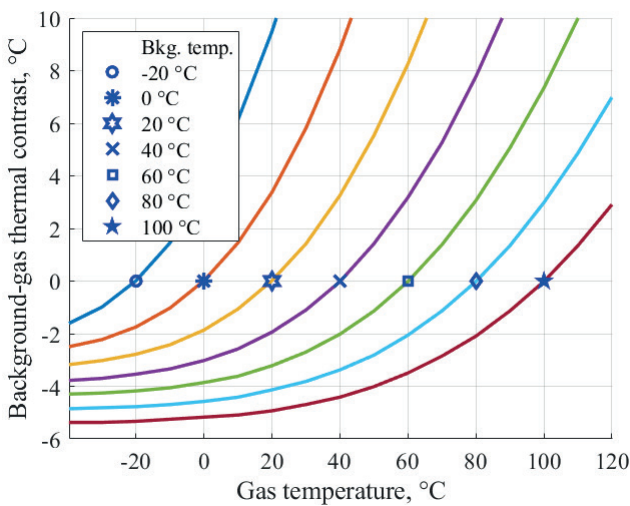
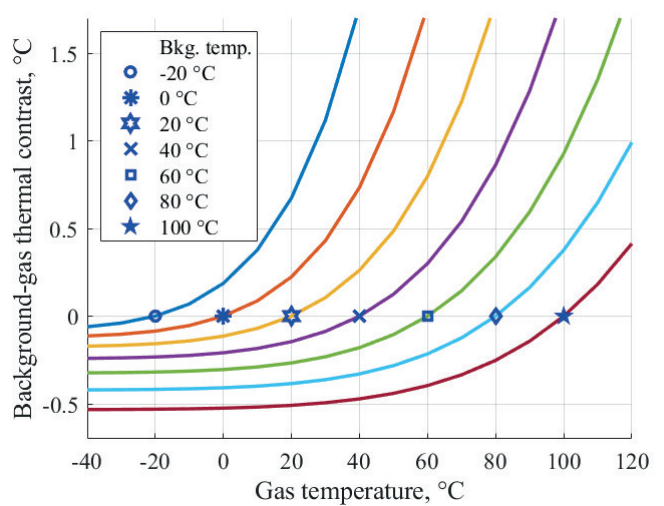
a)  $\text{CO}_2$ b)  $\text{CH}_4$ 

Fig. 4. Simulated thermal contrast between the background and gas plume, for different background and gas temperature combinations, for carbon dioxide (a) and methane (b), for a simulated cooled MWIR camera, with zero thermal contrast marks

Rys. 4. Symulowany kontrast termiczny między tłem a chmurą gazu dla różnych kombinacji fizycznych wartości temperatury tła i gazu, dla a) dwutlenku węgla oraz b) metanu, dla symulowanej chłodzonej kamery MWIR, z zaznaczonymi punktami zerowego kontrastu termicznego

## 4. Discussion

Simulation results presented in Fig. 4 demonstrate that a general purpose cooled thermographic camera (without bandpass filter) operating in the MWIR band (3–5  $\mu\text{m}$ ) can be successfully used for gas imaging. Assuming 100 %  $\text{CO}_2$  concentration and 1 cm path length (corresponding to 10 000 ppm · m), the temperature difference between gas and background equal to 10 °C translates to the thermal contrast of about 1 to 1.13 °C in images for background temperature from –20 °C to 100 °C, respectively. It strongly exceeds NETD of typical cooled camera (20 mK) and should provide clear gas imaging.

For methane with the same concentration, on the other hand, if the gas is colder by 10 °C than the background, one can expect thermal contrast of about 40–140 mK for background temperature from –20 °C to 100 °C, respectively. It is much closer to NETD, and one should expect much lower signal to noise ratio in the images than for  $\text{CO}_2$ .

In all cases, the probability of gas detection is highly correlated with scene thermal contrast between the gas and the background area. It will depend on gas type. If the thermal contrast drops to zero, or remains below the camera NETD parameter value, gas imaging will no longer be possible. Additionally, if the background temperature is very low, for example in winter, and one would like to image a cold gas leak in such conditions, a very low thermal contrast is expected, making leak detection difficult. In such conditions, an active solution may be considered [8] to actively increase thermal contrast.

On the other hand, if the scenario is reversed, i.e. hot gas is imaged against a cold background, one can expect better performance than for imaging cold gas against a hot background. The performance gain in this case is proportional to the difference of gas and background temperature. Let us take an example shown in Fig. 5, where two cases are marked. In one case  $\text{CO}_2$  gas at 0 °C is imaged against background at 100 °C, resulting in thermal contrast much lower than for imaging  $\text{CO}_2$  gas at 100 °C against background at 0 °C. This difference is due to non-linear camera radiometric response curve  $T(M)$ .

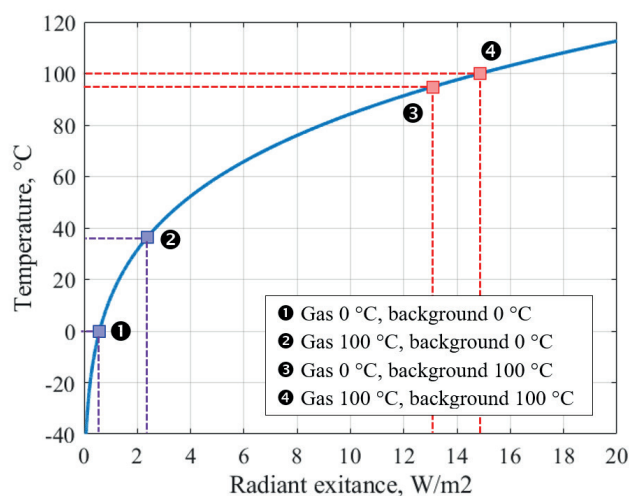


Fig. 5. Camera radiometric response curve  $T(M)$  with two thermal contrast cases marked

Rys. 5. Charakterystyka radiometrycznej odpowiedzi kamery  $T(M)$  z zaznaczonymi dwoma przypadkami kontrastu termicznego

## 5. Conclusions

The presented model demonstrates that during optical gas imaging one should use sensitive equipment, because the thermal contrast between the gas and background areas of the

scene can be very low. Especially in cold weather conditions, it could be advisable to increase the physical background-gas temperature difference using active solutions. Thanks to the presented model, one can estimate the chances of gas leak detection, knowing the gas type, its concentration, the optical path length in the gas plume and the temperature of the background and the leak.

## Bibliography

1. Olbrycht R., Kałuza M., Wittchen W., Borecki M., Więcek B., De Mey G., Kopeć M., *Gas identification and estimation of its concentration in a tube using thermographic camera with diffraction grating*, “Quantitative InfraRed Thermography Journal”, Vol. 15, No. 1, 2018, 106–120, DOI: 10.1080/17686733.2017.1385179.
2. Olbrycht R., Kałuza M., *Optical Gas Imaging With Uncooled Thermal Imaging Camera – Impact of Warm Filters and Elevated Background Temperature*, “IEEE Transactions on Industrial Electronics”, Vol. 67, No. 11, 2020, 9824–9832, DOI: 10.1109/TIE.2019.2956412.
3. Zimmerle D., Vaughn T., Bell C., Bennett K., Deshmukh P., Thoma E., *Detection Limits of Optical Gas Imaging for Natural Gas Leak Detection in Realistic Controlled Conditions*, “Environmental Science and Technology”, Vol. 54, 2020, 11506–11514, DOI: 10.1021/acs.est.0c01285.
4. Olbrycht R., *A novel method for sensitivity modelling of optical gas imaging thermal cameras with warm filters*, “Quantitative InfraRed Thermography Journal”, Vol. 19, No. 5, 2022, 331–346, DOI: 10.1080/17686733.2021.1962096
5. de Lima Filho G.M., Cardoso Fernandes de Almeida R., Morgado de Castro R., Damião A.J., *Operational Measurements for Infrared Camera Characterization*, “Journal of Aerospace Technology and Management”, Vol. 9, No. 4, 2017, 519–528, DOI: 10.5028/jatm.v9i4.589.
6. Le Touz N., Toullier T., Dumoulin J., *Infrared thermography applied to the study of heated and solar pavement: from numerical modeling to small scale laboratory experiments*, Proceedings SPIE 10214 – Thermosense: Thermal Infrared Applications XXXIX, 2017, Anaheim, United States, DOI: 10.1117/12.2262778.
7. Więcek P., Więcek B., *Performance analysis of dual-band microbolometer camera for industrial gases detection*, “Measurement Automation Monitoring”, Vol. 64, No. 04, 2018, 90–94, ISSN 2450-2855.
8. Barber R., Rodriguez-Conejo M.A., Melendez J., Garrido S., *Design of an Infrared Imaging System for Robotic Inspection of Gas Leaks in Industrial Environments*, “International Journal of Advanced Robotic Systems”, Vol. 16, 2015, DOI: 10.5772/60058.
9. FLIR Systems, Inc., *Spectral response curves of various photonic sensors*, [[https://flir.custhelp.com/app/answers/detail/a\\_id/3634/~spectral-response-curves-of-various-photonic-sensors](https://flir.custhelp.com/app/answers/detail/a_id/3634/~spectral-response-curves-of-various-photonic-sensors)]
10. HITRAN on the web – V.E. Zuev Institute of Atmospheric Optics (IAO), Tomsk, Russian Federation, [<https://hitran.iao.ru>].

## Other sources

# Model kontrastu termicznego do analizy skuteczności optycznego obrazowania gazów

**Streszczenie:** Artykuł przedstawia numeryczne modelowanie kontrastu termicznego w zastosowaniach do optycznego obrazowania gazów (ang. OGI). Fizyczna temperatura obrazowanej chmury gazu może być wyższa lub niższa od temperatury tła, a różnica ta stanowi niezbędny warunek detekcji. W zależności od rzeczywistego kontrastu termicznego pomiędzy chmurą gazu a tłem, mierzona różnica temperatur może przyjmować różne wartości. Idealnie kontrast ten powinien być możliwie jak największy, aby zapewnić wyraźną wizualizację chmury. W praktyce jednak należy dostosować się do rzeczywistych warunków oraz być w stanie przewidzieć oczekiwaną zmierzoną różnicę temperatur i porównać ją z wartością parametru NETD kamery (ang. Noise Equivalent Temperature Difference), aby oszacować stosunek sygnału do szumu. Zgodnie z wynikami przedstawionymi w pracy, skutek łącznego wpływu prawa Plancka, radiometrycznej charakterystyki kamery oraz widm absorpcji gazów, mierzony kontrast termiczny silnie zależy od bezwzględnych wartości fizycznych temperatury zarówno gazu, jak i tła — a nie jedynie od różnicy wartości temperatury między nimi.

**Słowa kluczowe:** termowizja, optyczne obrazowanie gazów, kamera, kontrast termiczny

## Robert Olbrycht, DSc PhD Eng.

robert.olbrycht@p.lodz.pl

ORCID: 0000-0001-9842-2815



In 2025, he received the DSc degree from Lodz University of Technology. His research focuses on thermographic methods of optical gas imaging for detecting unwanted gas emissions. He is affiliated with the Institute of Electronics at Lodz University of Technology, where he conducts research on thermal imaging camera modelling, non destructive testing, and cultural heritage protection. His work includes the design and development of specialized thermal imaging systems for advanced applications. He is the co author of numerous scientific publications and books in the fields of thermography and infrared spectrometry. He also teaches professional thermography courses and serves on the Organizing Committee of the Infrared Thermography and Thermometry Conference.